taining a participating, heat-generating gas, *J. Heat Transfer* **83**, 199–206 (1961).
2. Y. S. Chou and C. L. Tien, A modified moment method for radiative transfer in non-planar systems, *J. Quant. Spectrosc. Radiat. Transfer* **8**, 919–933 (1968).
3. B. L. Hunt, An examination of the method of regional averaging for radiative transfer between concentric spheres, *Int. J. Heat Mass Transfer* **11**, 1071–1076 (1968).
4. R. Viskanta and A. L. Crosbie, Radiative transfer through a spherical shell of an absorbing-emitting gray medium, *J. Quant. Spectrosc. Radiat. Transfer* 7, 871–889 (1967).
5. I. L. Ryhming, Radiative transfer between two concentric spheres separated by an absorbing and emitting gas, *Int. J. Heat Mass Transfer* **9**, 315–324 (1966).
6. G. Emanuel, Application of matched asymptotic expansions to radiative transfer in an optically thick gas, Aerospace Corp. Report TR-0158(3240-20)-14 (1968).
7. R. F. Chisnell, Radiant heat transfer in a spherically symmetric medium, *AIAA Jl* **6**, 1389–1391 (1968).
8. D. B. Olfe, Application of a modified differential approximation to radiative transfer in a gray medium between concentric spheres and cylinders, *J. Quant. Spectrosc. Radiat. Transfer* **8**, 899–907 (1968).
9. R. E. Marshak, The variational method for asymptotic neutron densities, *Phys. Rev.* **71**, 688–693 (1947).

black cylinder upon the neutron density in an infinite non-capturing medium, *Proc. Phys. Soc.* A, **64**, 881–902 (1951).
11. B. Davison, *Neutron Transport Theory*. Section 5.3. Clarendon Press, Oxford (1958).
12. G. Emanuel, Radiative energy transfer from a small sphere, Aerospace Corp. Report, TR-0200(4240-20)-1 (1968).
13. K. M. Case and P. F. Zweifel, *Linear Transport Theory*, p. 138, $c = 1{\cdot}0$ column. Addison-Wesley, Reading, Massachusetts (1967).
14. G. Emanuel, Radiative transport in an optically thick planar medium, *Int. J. Heat Mass Transfer* **11**, 1413–1416 (1968).
15. V. Kourganoff, *Basic Methods in Transfer Problems*, p. 138. Dover Publications, New York (1963).
16. M. A. Heaslet and B. Baldwin, Close analogy between radiative and conductive heat flux in a finite slab, *AIAA Jl* **2**, 2180–2186 (1964).
17. D. B. Olfe, A modification of the differential approxi- for radiative transfer, *AIAA Jl* **5**, 638–643 (1967).

Int. J. Heat Mass Transfer. Vol. 12, pp. 1331–1337. Pergamon Press 1969. Printed in Great Britain

TRANSIENT RADIATIVE HEAT TRANSFER IN A PLANE LAYER

K. KRISHNA PRASAD† and **R. G. HERING**

University of Illinois at Urbana-Champaign, Urbana, Illinois, U.S.A.

(*Received* 12 *August* 1968 *and in revised form* 5 *February* 1969)

INTRODUCTION

Energy transfer by thermal radiation within absorbing and emitting media has received considerable attention in recent years. Transient radiative transfer processes, however, have received only limited consideration. This study is concerned with unsteady energy transfer by radiation in a stationary plane layer of a non-conducting medium. Nemchinov [1] utilized a two-flux model to study transient cooling of a layer in the absence of walls while Viskanta and Bathla [2] employed an exact formulation to study the same system when the layer is symmetrically heated by an external diffuse and collimated radiant flux. The latter authors also cite a number of other transient radiative transfer studies most of which are concerned with a spherical geometry. The present study is distinguished from earlier investigations by the presence of walls and unsymmetrical boundary conditions. The system with the conditions imposed here is analogous to the conventional problem in heat conduction and, therefore, permits ready comparison with results for simultaneous conductive and radiative transfer. Exact radiative transfer methods are employed to formulate the energy transfer problem and two techniques are developed to construct solutions to the governing energy equation.

† Present address: Department of Mechanical Engineering, Indian Institute of Science, Bangalore-12, India.

ANALYSIS

Consider a plane parallel layer of a non-scattering gray medium confined between uniform temperature black planes (see insert in Fig. 1). Postulating a purely radiating medium and neglecting ionization and dissociation effects, the energy equation for the medium may be written as

$$\rho c_v \frac{\partial T}{\partial t} = -\frac{\partial F}{\partial x} \tag{1}$$

where T, F, t, and x denote the local absolute temperature, local radiative flux, time, and space coordinate, respectively. The symbols ρ and c_v designate the mass density and the constant volume specific heat of the enclosed medium. In writing equation (1), plane symmetry has been assumed and radiation energy density neglected in comparison to molecular energy density. Physically, equation (1) equates the instantaneous net radiative energy transport rate to a unit volume element to the time rate of increase of the molecular energy of the element. For black walls the local radiative flux is

$$F(\tau, t) = 2\sigma\Big[T_0^4(t)\,E_3(\tau) - T_1^4(t)\,E_3(\tau_0 - \tau) + \int_0^{\tau_0} T^4(\tau', t)\,E_2(|\tau - \tau'|)\,\mathrm{sign}\,(\tau - \tau')\,\mathrm{d}\tau'\Big] \tag{2}$$

with $T_0(t)$ and $T_1(t)$ the time dependent temperatures of the lower ($\tau = 0$) and upper wall ($\tau = \tau_0$), respectively. The symbols σ, $\tau(= \kappa x)$, and $\tau_0(= \kappa x_0)$ denote the Stefan–Boltzmann radiation constant, the optical distance measured from the lower wall and the optical thickness of the layer, respectively. $E_n(\tau)$ is the well-known exponential integral function of order n. Differentiation of the flux expression and subsequent substitution into the energy equation gives

$$\rho c_v \frac{\partial T}{\partial t} = 2\kappa\sigma\left[T_0^4(t)\,E_2(\tau) + T_1^4(t)\,E_2(\tau_0 - \tau) + \int_0^{\tau_0} T^4(\tau', t)\,E_1(|\tau - \tau'|)\,\mathrm{d}\tau' - 2T^4(\tau, t)\right]. \tag{3}$$

Equation (3) governs the temperature distribution in a radiating non-scattering, gray gas confined between black walls for arbitrary optical thickness, arbitrary initial temperature distribution and arbitrary variation of the wall temperatures with time. Solutions are presented later for an initial state of uniform temperature T_1 when the lower wall ($\tau = 0$) undergoes a step increase in temperature to T_0. The upper wall ($\tau = \tau_0$) remains at the initial temperature of the layer. These wall conditions were chosen to correspond to the extensive results available [3, 4] for steady radiative transfer in a plane layer confined between unequal temperature walls. For future reference, the energy and flux equations corresponding to the imposed conditions are presented in dimensionless form.

$$\frac{\partial \theta}{\partial t^*} = \tfrac{1}{2}\Big[E_2(\tau) + \theta_1^4 E_2(\tau_0 - \tau) + \int_0^{\tau_0} \theta^4(\tau', t)\,E_1(|\tau - \tau'|)\,\mathrm{d}\tau' - 2\theta^4(\tau, t^*)\Big]. \tag{4}$$

The initial condition is given by

$$\theta(\tau, 0) = \theta_1. \tag{5}$$

The corresponding flux expression is

$$F^* = \tfrac{1}{2}\Big[E_3(\tau) - \theta_1^4 E_3(\tau_0 - \tau) + \int_0^{\tau_0} \theta^4(\tau', t^*)\,E_2(|\tau - \tau'|)\,\mathrm{sign}\,(\tau - \tau')\,\mathrm{d}\tau'\Big]. \tag{6}$$

The dimensionless variables introduced are defined as follows.

$$\theta = \frac{T}{T_0}, \quad \theta_1 = \frac{T_1}{T_0}, \quad F^* = \frac{F}{4\sigma T_0^4}, \quad t^* = \frac{4\kappa\sigma T_0^3}{\rho c_v} t. \tag{7}$$

The parameter $\rho c_v/\kappa\sigma T_0^3$ introduced in the dimensionless time variable, t^*, characterizes the time required to radiate the entire internal energy of the medium of temperature T_0 at a rate determined by this same temperature.

NUMERICAL SOLUTION TO THE ENERGY EQUATION

The energy equation (4), is a nonlinear, integro-differential equation for which analytical closed form solutions do not appear possible and, therefore, numerical methods were employed. The numerical solution is complicated by the fact that $E_1(|\tau - \tau|)$ is singular at the origin even though the integral exists and is finite. To circumvent this difficulty, the integral was evaluated by a functional approximation technique. The function $\theta^4(\tau, t^*)$ was approximated by a finite expansion in polynomials orthogonal over a set of preselected space grid points, distributed in a suitable manner in the interval under consideration. Thus

$$\theta^4(\tau, t^*) = \sum_{j=0}^{k} B_j(t^*)\,P_j(\tau) \tag{8}$$

where $P_j(\tau)$ denotes the orthogonal polynomial of order j. The orthogonal polynomials were constructed by adapting an algorithm suggested by Anderson [5] to the discrete situation. The time dependent coefficients $B_j(t^*)$ were evaluated at each instant of time according to a least-squares procedure given by Forsythe [6].

Spatial discretization of equation (4) and subsequent use of the polynomial approximation yields a system of simultaneous ordinary differential equations with the initial condition prescribed by equation (5). Standard numerical integration techniques were employed to numerically solve the resulting set of equations [7]. The accuracy of the solution method was investigated by independent error studies of the least squares polynomial approximation and the numerical integration technique. Comparisons to reported steady state results [4] showed agreement to better than 1 per cent in most cases investigated. The transient results are estimated to be at least of this accuracy.

RESULTS AND DISCUSSION

Transient temperature and flux distributions have been evaluated for a medium initially at a uniform temperature T_1 when the temperature of the lower black wall is suddenly increased to and thereafter maintained at temperature T_0. The upper wall remains at the initial temperature T_1. The dimensionless temperature distribution at each instant of dimensionless time t^* depends on the optical thickness τ_0 and the temperature ratio θ_1. Since θ_1 is the ratio of cold wall to hot wall temperature, a decrease in θ_1 for fixed initial temperature corresponds to an increase in temperature change of the hot wall. A convenient presentation of results is afforded by the dimensionless variables θ and $\mathscr{F}$ defined by

$$\theta = \frac{\theta^4 - \theta_1^4}{1 - \theta_1^4}, \qquad \mathscr{F} = \frac{4F^*}{1 - \theta_1^4}. \tag{9}$$

Both θ and $\mathscr{F}$ are independent of θ_1 at steady state and available steady state results [3, 4] are presented in terms of these quantities. At steady state $\mathscr{F}$ is uniform across the layer and θ is asymmetric about the mid-plane.

The influence of optical thickness on the temperature and flux distributions during heating is illustrated in Fig. 1 for a θ_1 value of 0·5. Distributions are presented at selected values of dimensionless time for optical thickness values of 0·1, 1·0 and 10·0. The phenomenon of temperature slip is evident in all temperature distributions and is attributed to the absence of any molecular transport mechanism, such as heat conduction, which requires temperature continuity at the wall-gas boundary. For the smallest value of optical thickness, $\tau_0 = 0{\cdot}1$, the temperature and flux distributions are nearly uniform across the layer and, furthermore, the radiant flux is large. These characteristics point to the approach of the layer to the optically thin

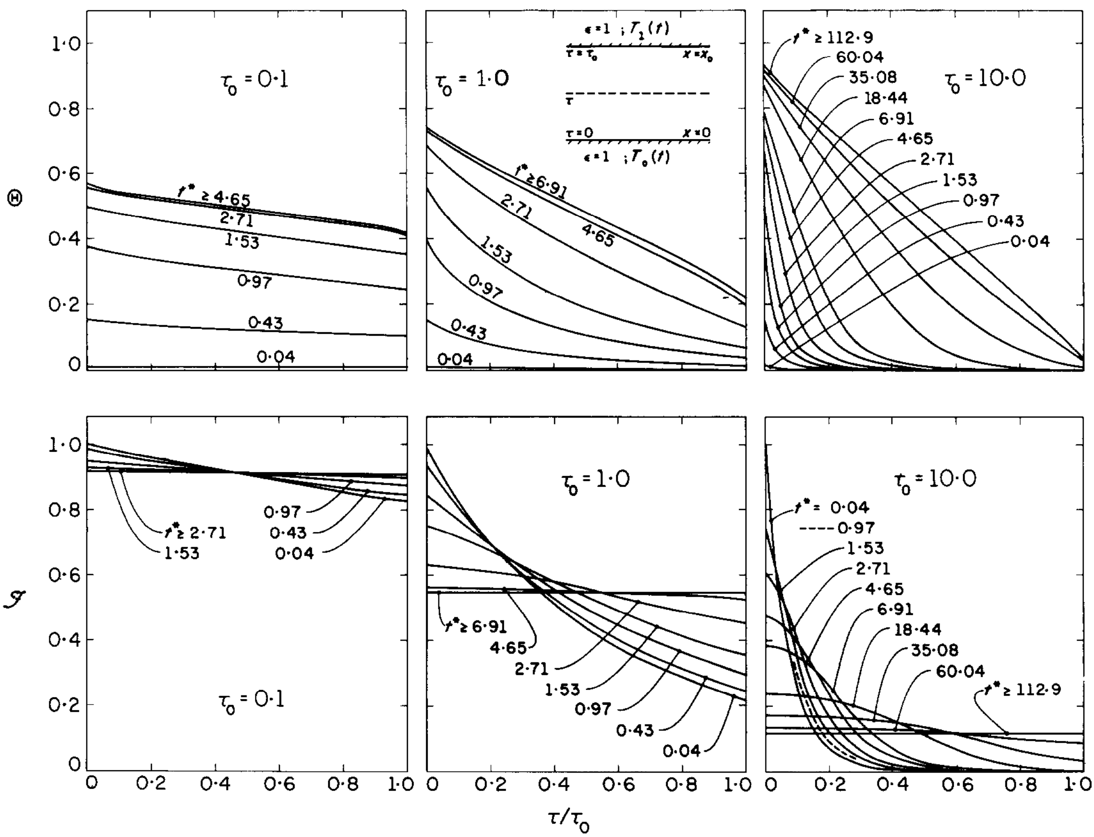

FIG. 1. Effect of optical thickness on temperature and flux distributions; $\theta_1 = 0{\cdot}5$.

limit ($\tau_0 \ll 1$) at which the temperature throughout the layer uniformly changes with time and flux is constant at a value near unity. On the other hand, the temperature and flux distributions for $\tau_0 = 10{\cdot}0$ exhibit large gradients and are reminiscent of those commonly observed in transient diffusion phenomena. These characteristics are attributed to the fact that at $\tau_0 = 10{\cdot}0$ the layer is approaching the optically thick limit ($\tau_0 \gg 1$) where each gas volume is significantly influenced only by its immediate neighbors and, consequently, the radiative transfer process acquires a diffusive character. The distributions for $\tau_0 = 1{\cdot}0$ display characteristics intermediate to those for the smaller and the larger optical thickness values.

The response of the medium to the change in wall temperature is illustrated by the results presented in Figs. 2 and 3. There is shown the variation with time of boundary temperatures and fluxes, respectively, for $\theta_1 = 0{\cdot}5$. The trends of increasing non-uniformity in temperature and diminishing flux values with increasing optical thickness are also evident here. It may be observed that the response of both temperature and flux for the smaller optical thickness values is of the same order while that for $\tau_0 = 10{\cdot}0$ is slower by an order of magnitude. Furthermore, while temperature and flux at both boundaries for $\tau_0 = 0{\cdot}1$ and $1{\cdot}0$ respond immediately to the wall temperature change, a considerable time elapses for $\tau_0 = 10{\cdot}0$ before the temperature and flux at the cold boundary show any significant change from their initial value. This points to the large impedance to radiant energy transfer inherent in the

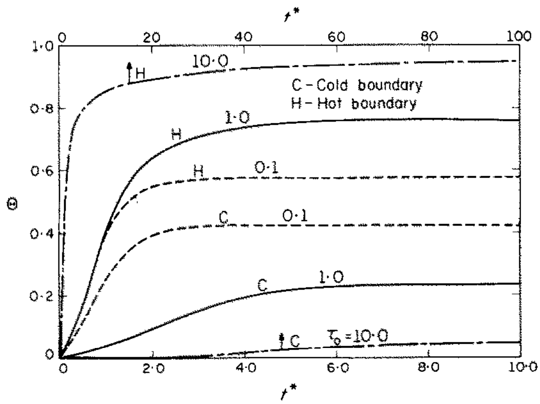

FIG. 2. Effect of optical thickness on time variation of boundary temperatures; $\theta_1 = 0{\cdot}5$.

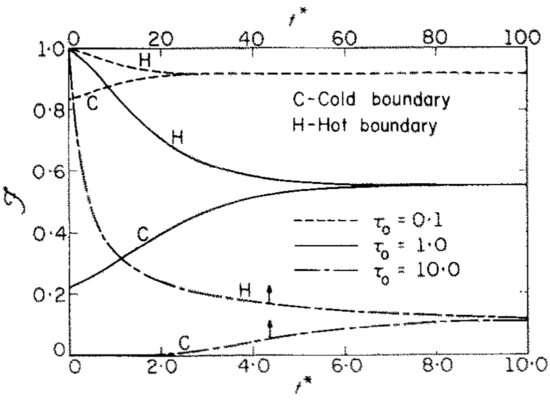

FIG. 3. Effect of optical thickness on time variation of boundary fluxes; $\theta_1 = 0{\cdot}5$.

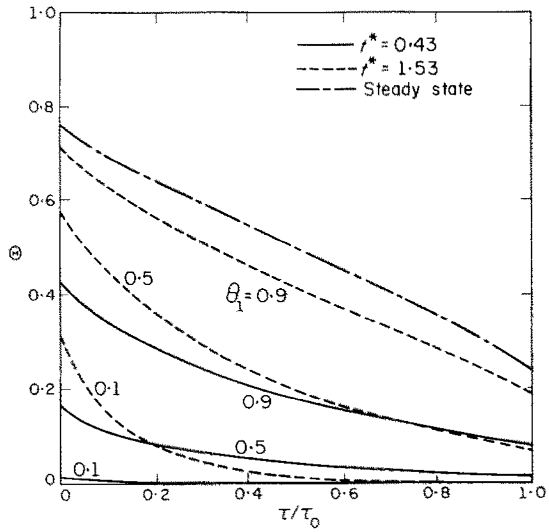

FIG. 4. Effect of θ_1 on temperature distributions: $\tau_0 = 1{\cdot}0$.

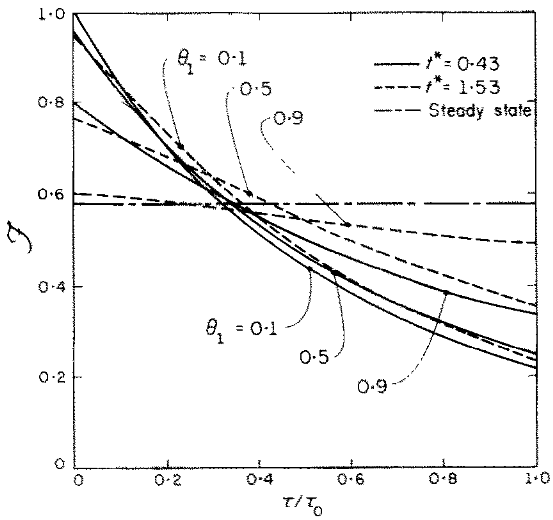

FIG. 5. Effect of θ_1 on flux distributions; $\tau_0 = 1{\cdot}0$.

diffusion mechanism dominant at $\tau_0 = 10{\cdot}0$. Finally, the results of these figures clearly establish that, in dimensionless time t^*, the layer with the smallest value of optical thickness heats the fastest and the response of the medium is retarded as the optical thickness of the layer increases.

The influence of the magnitude of the wall temperature change on temperature and flux distributions is illustrated in Figs. 4 and 5 at selected times for an optical thickness value of unity. As expected, the θ_1 value does not significantly affect the general characteristics of the temperature and flux distributions and this observation holds also for the results at other values of optical thickness. The effect of an increase in temperature change of the lower wall for fixed initial layer temperature is a retardation of the response of the medium to the driving flux. This is clearly demonstrated in Fig. 6 where the variation with time of the boundary temperature and fluxes is shown for $\tau_0 = 1{\cdot}0$.

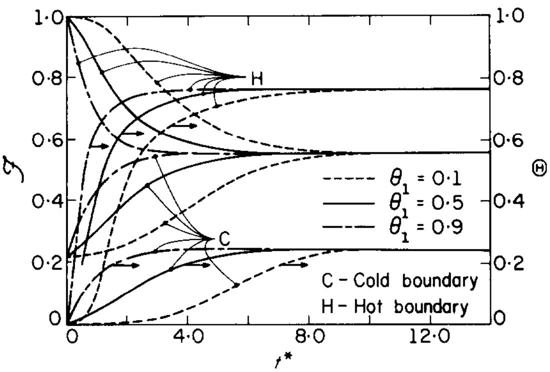

FIG. 6. Effect of θ_1 on time variation of boundary temperatures and boundary fluxes; $\tau_0 = 1{\cdot}0$.

The previous discussion concerning the influence of the dimensionless parameters τ_0 and θ_1 on the transient heating of the layer was based on the dimensionless time variable t^*. It is important to interpret the trends in terms of physical time t. For this purpose consider a gas layer of fixed thermal properties (ρ, c_v), fixed physical thickness (x_0), and fixed initial temperature (T_1). Then $t\alpha(\theta_1^3 t^*/\tau_0)$ and inspection of the foregoing results in light of this relation reveals the following. First, on a real time basis, an increase in the temperature change of the lower wall for a fixed value of optical thickness increases the response rate of the layer. On physical grounds, this trend is quite plausible. Second, the layer with optical thickness unity heats fastest and the layer with optical thickness 0·1 heats slowest. The heating is slower for $\tau_0 = 0{\cdot}1$ than for $\tau_0 = 1{\cdot}0$ because the former has a relatively lower absorption coefficient and therefore absorbs comparitively less energy. On the other hand, the diffusion mechanism dominant at $\tau_0 = 10{\cdot}0$ is inherently a slow transport process in comparison to the global interaction mechanism prevailing at $\tau_0 = 1{\cdot}0$. It is somewhat surprising, however, to find that the time required to attain steady state conditions is considerably less for the diffusion process at large optical thickness than that for $\tau_0 = 0{\cdot}1$. This must be attributed to the lack of significant interaction between the radiation and matter at the low value of optical thickness.

SOLUTION BY THE METHOD OF MOMENTS

The numerical method of solution to equation (4) presented earlier is accurate but requires a large amount of computation time. It is therefore, desirable to seek other methods of solution which can yield results with less effort at the expense of some accuracy. The method of moments is an approximate technique which has enjoyed some success and when applied to the problem at hand significantly reduces the computational effort. The method is variational in character and has been discussed in detail with regard to the determination of approximate solutions to integral equations [8, 9] and nonlinear partial differential equations [10].

It is convenient for the present purpose to compactly write equation (4) in the form

$$L[\theta(\tau, t^*)] - f(\tau) = 0 \qquad (10)$$

where the operator L and function f are defined as follows.

$$\left.\begin{aligned} L[\theta(\tau, t^*)] &\equiv \frac{\partial \theta}{\partial t^*} - \frac{1}{2}\int_0^{\tau_0} \theta^4(\tau', t^*)\, E_1(|\tau - \tau'|)\, d\tau' \\ &\qquad + \theta^4(\tau, t^*) \\ f(\tau) &\equiv \tfrac{1}{2}\{E_2(\tau) + \theta_1^4 E_2(\tau_0 - \tau)\}. \end{aligned}\right\} \qquad (11)$$

The initial condition is equation (5).

An approximate solution to the energy equation, $\phi(\tau, t^*)$, is sought in the following form

$$\Phi(\tau, t^*) \equiv \sum_{j=0}^{N} \phi_j(t^*)\, \tau^j \qquad (12)$$

where the $\phi_j(t^*)$ are as yet undetermined functions. A residual, $R[\phi_j(t^*), \tau]$, corresponding to the assumed solution is defined as

$$R[\phi_j(t^*), \tau] = L[\Phi(\tau, t^*)] - f(\tau). \qquad (13)$$

From a comparison of equations (13) and (10) it follows that the residual is generally non-vanishing in the domain of integration except for the exact solution. The functions $\phi_j(t^*)$ are now chosen to make the residual small in some sense. For this purpose the method of moments requires the first $N + 1$ moments of the residual to vanish; that is, we require that

$$\int_0^{\tau_0} \tau^i R[\phi_j(t^*), \tau]\, d\tau = 0 \qquad (i = 0, 1, 2, \ldots, N). \qquad (14)$$

This procedure generates a system of $N + 1$ simultaneous nonlinear ordinary differential equations for the $\phi_j(t^*)$ which may be written as

$$\sum_{j=0}^{N} a_{ij}\frac{d\phi_j}{dt^*} + \sum_{j=0}^{4N} C_{ij}U_j(t^*) = F_i \tag{15}$$

where

$$a_{ij} = \tau_0^{i+j+1}/(i + j + 1)$$

$$C_{ij} = \tfrac{1}{2}\int_0^{\tau_0} \tau^i\,d\tau \int_0^{\tau_0} (\tau')^j E_1(|\tau - \tau'|)\,d\tau' - a_{ij} \tag{16}$$

$$F_i = \int_0^{\tau_0} \tau^i f(\tau)\,d\tau.$$

The coefficients a_{ij} and C_{ij} depend only on optical thickness of the medium while F_i depends on both optical thickness and θ_1. The integrals in C_{ij} and F_i may be evaluated in closed form and the results expressed in terms of exponential integral functions of orders higher than unity. Thus, the singularity present in equation (4) is eliminated. The resulting lengthy expressions are available elsewhere [7] and are not presented here. The functions denoted $U_j(t^*)$ are combinations of the $\phi_j(t^*)$ and are defined by the following relation

$$\Phi^4(\tau, t^*) = \left(\sum_{j=0}^{N} \phi_j(t^*)\,\tau^j\right)^4 = \sum_{j=0}^{4N} U_j(t^*)\,\tau^j. \tag{17}$$

The initial conditions for ϕ_j can be determined by a similar procedure applied to equation (5). In the present application, however, they may be written by inspection of equations (12) and (5) as

$$\phi_0(0) = \theta_1,\ \phi_j(0) = 0 \qquad (j = 1, 2, \ldots, N). \tag{18}$$

The system of equations expressed by equation (15) with the initial conditions above were numerically integrated and solutions were obtained with five to six times less computation time than that required for the numerical solution.

COMPARISON OF RESULTS

Temperature distributions were evaluated using the moment method with $N = 4$. A marked improvement in accuracy was observed when N was increased from 3 to 4, but very little thereafter. The moment method failed to give physically meaningful solutions for $\tau_0 \geq 5$. This failure is attributed to the choice of power functions (τ^j) to describe the spatial dependence of temperature. At large optical thickness values, the temperature variation with distance is exponential in character and cannot be adequately approximated by the selected functions. The errors introduced by the approximation are sufficient to cause an unstable numerical integration. The results obtained for the temperature and flux distributions with $\tau_0 \leq 2$, however, exhibited all the features previously discussed in connection with the numerical solution and, therefore, we turn our attention to the accuracy of the moment results.

The accuracy of the moment results for temperature and flux was investigated by comparison of the results to those evaluated by the numerical method. Figure 7 shows the typical per cent error in local temperature at selected values of t^* for $\tau_0 = 1{\cdot}0$. This figure indicates that the moment results at each instant of time oscillated about the numerical result. Except at very early times when the cold boundary usually exhibited low temperatures, the moment results gave low temperature values at the hot boundary and high temperature values at the cold boundary. Although the cold boundary temperature at early times was sometimes in error by a factor of two, the accuracy of the moment results improved as time progressed and generally showed agreement within 1 per cent at interior points and intermediate times. The greatest temperature errors occurred at the boundaries with discrepancies of over 8 per cent at steady state. The accuracy of the moment results for temperature were not significantly affected by the value of θ_1. The most accurate results for temperature were obtained at an optical thickness value of unity, the exceptions being the cold boundary temperature and early time results. The radiant flux distributions evaluated with the moment method temperature distributions showed agreement with those of the numerical solution to four significant figures in almost all cases investigated.

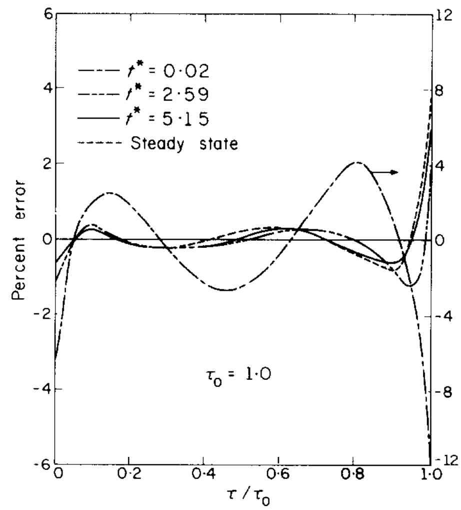

FIG. 7. Typical error in temperature by moment method; $\tau_0 = 1{\cdot}0$, $\theta_1 = 0{\cdot}5$.

ACKNOWLEDGEMENTS

One of the authors (K. Krishna Prasad) would like to gratefully acknowledge the support of USAID, Washington, D.C., and the authorities of Indian Institute of Science, Bangalore, India, for making this study possible.

REFERENCES

1. I. V. Nemchinov, Some non-stationary problems of radiative heat transfer, *Zh. Prinkl. Mekh. Tekh. Fiz.* 36–57 (1960).
2. R. Viskanta and P. S. Bathla, Unsteady energy transfer in a layer of gray gas by thermal radiation, *Z. Angew. Math. Phys.* **18**, 353–367 (1967).
3. C. M. Usiskin and E. M. Sparrow, Thermal radiation between parallel plates separated by an absorbing-emitting non-isothermal gas, *Int. J. Heat Mass Transfer* **1**, 28–36 (1960).
4. M. A. Heaslet and R. F. Warming, Radiative transport and wall temperature slip in an absorbing planar medium, *Int. J. Heat Mass Transfer* **8**, 979–994 (1965).
5. D. G. Anderson, Gaussian quadrature formulae for $\int_0 - \ln(x)f(x)\,dx$, *Math. Computation* **19**, 477–481 (1965).
6. G. E. Forsythe, Generation and use of orthogonal polynomials for data-fitting on a digital computer, *J. Soc. Ind. Appl. Math.* **5**, 74–88 (1957).
7. K. Krishna Prasad, Unsteady radiant heat transfer in stationary media, Ph.D. Thesis, University of Illinois (1966).
8. L. V. Kantorovich and V. I. Krylov, *Approximate Methods of Higher Analysis*, p. 150. Noordhoff, Groninger, The Netherlands (1958).
9. I. S. Berezin and N. P. Zhidkov, *Computing Methods*, Vol. 2. Pergamon Press, New York (1965).
10. W. F. Ames, *Non-Linear Partial Equations in Engineering*, p. 249. Academic Press, New York (1965).